CIRP Annals - Manufacturing Technology 00 (2022) 1–4

Contents lists available at ScienceDirect

CIRP Annals - Manufacturing Technology

journal homepage: https://www.editorialmanager.com/CIRP/default.aspx

Modal parameter recovery from temporally aliased video recordings of cutting tools

Mohit Law[a,*], Rohit Lambora[a], Anshid Nuhman P[a], Suparno Mukhopadhyay[b]

[a] Machine Tool Dynamics Laboratory, Department of Mechanical Engineering, Indian Institute of Technology Kanpur, India
[b] Department of Civil Engineering, Indian Institute of Technology Kanpur, India

Submitted by Toshimichi Moriwaki (1), Kobe, Japan

ARTICLE INFO

Article history:
Available online xxx

Keywords:
Dynamics
Cutting tool
Aliased signals

ABSTRACT

Vision-based modal analysis methods are non-contact, do not require data acquisition systems, and facilitate full-field shape analysis. Leveraging these advantages for industrial use is precluded by the need for expensive high-speed cameras. This paper presents new methods to recover modal parameters from potentially temporally aliased video recordings of cutting tools using economical medium-speed cameras. Folding properties of fractionally uncorrelated aliased signals are used together with the eigensystem realization algorithm to recover modal parameters from tool motion extracted using image processing schemes. Results agree with those from accelerations sampled properly. Methods are generalized for use with other sensors.

1. Introduction

Performance of machine tool systems depends on its dynamics characterized by modal parameters [1]. The fidelity with which modal parameters can be estimated depends on how vibration signals are sampled. Measurements usually respect the Nyquist limit to avoid aliasing. This is easy enough with modern transducers, analog to digital converters, and data acquisition systems. However, respecting the Nyquist limit for newer vision-based modal analysis methods that extract modal parameters from motion registered from video recordings of vibrating tools using image processing techniques requires the use of high-speed and high spatial resolution cameras [2,3]. These cameras are expensive, costing between tens and hundreds of thousands of US dollars, and hence are not accessible for easy use. Since vision-based methods are non-contact in nature and facilitate full-field modal analysis, measurement setups are agile and do not require sophisticated data acquisition systems. Methods also do not suffer from mass-loading effects. Vision-based methods hence offer advantages over the use of traditional experimental modal analysis approaches [2–4]. However, since most digital cameras can record video at relatively low frame rates, and since vibration frequencies of cutting tools can range from a few tens of Hz to a few kHz, to leverage visual vibrometry's potential for industrial use, this paper presents novel methods to recover modal parameters from possibly temporally aliased video recordings of vibrating tools.

In the context of recovering data from incomplete observations for modal analysis, the emerging compressed sensing technique that can exactly recover a sparse signal from far fewer random samples than required by the Nyquist limit has found favour in structural health monitoring of civil infrastructure [5,6]. In other exemplary work, compressed sensing was successfully used to identify dynamics from video recordings of structures [7,8]. However, since availability of compressed sensing hardware samplers is still nascent, prior implementations acquired signals at uniform rates respecting the Nyquist limit, and post-processed to randomly down-sample. Since the present work aims to recover parameters from camera recordings that may or not be aliased, compressed sensing is not suited for the present application.

Other relevant work demonstrated recovery of natural frequencies [9] and deflection shapes from video recordings below the Nyquist rate by assuming that the signal is characterized by a single known frequency component. However, since cutting tools can potentially vibrate in many modes, and since those frequencies are not known a priori, methods proposed in [9] too are not suitable for our application of interest. Other seminal work exploited the signal aliasing and folding properties and the spatiotemporal uncoupling property of modal expansion to recover modal parameters from sub-Nyquist rate video recordings [10]. Though the method was shown to work well, it was demonstrated on laboratory-based bench-scale structures vibrating with large amplitudes and low frequencies, but with using video down-sampled from original high-speed recordings.

Since prior modal parameter recovery methods [5–10] are not directly applicable to tools that vibrate with small motion over a wide frequency range, this paper presents new methods to recover modal parameters from potentially temporally aliased video recordings. Methods proposed herein are illustrated on an end mill and a boring bar, both with multiple modes. Response of tools to an impulse excitation is recorded using a high resolution economical medium-speed camera that costs ~6000 US dollars, and samples at 960 and 1000 frames per second. Motion is registered using edge detection and tracking schemes [2–4]. To extract modal parameters from the potentially aliased response signal, we prefer to use the eigensystem realization algorithm (ERA) [11,12]. ERA readily allows

* Corresponding author.
E-mail address: mlaw@iitk.ac.in (M. Law).

https://doi.org/10.1016/j.cirp.2022.03.023
0007-8506/

for spatial-temporal decoupling and can be applied to possibly aliased signals to obtain the aliased frequencies, mode shapes and damping ratios, thus making parameter estimation simpler than other methods that relied on a combination of methods [10]. Folding properties of fractionally uncorrelated aliased signals are used to recover true parameters from observed ones. Methods are benchmarked with those from accelerations sampled at 51.2 kHz. Proposed methods, we believe, are the first such implementation of recovering machine tool modal parameters from signals sampled below the Nyquist rate.

The remainder of the paper is organized as follows. Section 2 outlines the theory of modal parameter recovery from potentially temporally aliased vibration measurements. Section 3 discusses the experimental setup and considerations. Results are discussed in Section 4. Main conclusions and outlook follow in Section 5.

2. Modal parameter recovery from vibration measurements

Consider that the system dynamics can be described by a first order continuous time state space model. If, for this system, the displacement response is $\mathbf{y}(t) = \mathbf{x}(t)$, and if $\mathbf{z}(t) = \begin{Bmatrix} \mathbf{x}(t) & \dot{\mathbf{x}}(t) \end{Bmatrix}^T$ is the state vector, then, the state and output equations are:

$$\dot{\mathbf{z}}(t) = \mathbf{A}_c\mathbf{z}(t) + \mathbf{B}_c\mathbf{u}(t)$$

$$\mathbf{y}(t) = \mathbf{C}_c\mathbf{z}(t) + \mathbf{D}_c\mathbf{u}(t), \tag{1}$$

wherein $\mathbf{A}_c$ is the state matrix, $\mathbf{B}_c$ is the input matrix, $\mathbf{u}(t)$ is the input force, $\mathbf{C}_c$ is the output matrix, and $\mathbf{D}_c$ is the feedthrough matrix. The eigenvalues, λ_j of $\mathbf{A}_c$ of an even order are [13]:

$$\lambda_j = -\zeta_j\omega_j \pm i\omega_j\sqrt{1-\zeta_j{}^2}, \tag{2}$$

wherein ω_j and ζ_j are the natural frequencies and damping ratios for mode j.

Since it is of interest to recover modal parameters from a discrete time representation, $\mathbf{y}(k\Delta t)$, wherein k is the sample number, and Δt, the sampling period, and if the signal is properly sampled respecting the Nyquist limit, i.e., if the sampling frequency, f_s is set to be at least $\geq 2f_m$, wherein f_m is the frequency of interest, then it is not difficult to show that the discrete time state matrix becomes [13]: $\mathbf{A}_d = \mathrm{e}^{\mathbf{A}_c\Delta t}$, and that the eigenvalues of $\mathbf{A}_d$ are, $\lambda_{dj} = \mathrm{e}\ ^{\lambda_j\Delta t}$. However, if sampling does not necessarily respect the Nyquist limit, then the eigenvalues of $\mathbf{A}_d$ may become:

$$\lambda_{dj} = \mathrm{e}^{\ \lambda_j\Delta t \pm i\ 2n\pi}, \tag{3}$$

wherein $2n\pi$ represents possible aliasing, with n being any non-negative integer. Substituting for λ_j in Eq. (3), and rearranging using $\Delta t = 1/f_s$, and $2\pi f_j = \omega_j$, Eq. (3) becomes:

$$\lambda_{dj} = \mathrm{e}^{\ 2\pi\Delta t\left(-\zeta_j f_j \pm if_j\sqrt{1-\zeta_j{}^2} \pm inf_s\right)}. \tag{4}$$

The discrete time eigenvalues are evidently a function of the sampling frequency. For the sampling frequency of interest, we identify the eigenvalues using the eigensystem realization algorithm [11]. For which, at first a Hankel matrix is constructed from the estimated discrete response $\mathbf{y}(k\Delta t)$ from video recordings of the vibrating tool. A singular value decomposition of the Hankel matrix is then performed to reorder the system to retain only the dominant modes of the system. Based on the reordering, a truncated observability matrix and a shifted Hankel matrix is constructed, which in turn is used to construct a discrete system realization of the system matrix, $\mathbf{A}_d$. The eigenvalues (λ_{dj}) and the complex valued eigenvectors (ψ_{dj}) are obtained from $\mathbf{A}_d$. For details on the ERA implementation, please see [11,12].

The resulting observed natural frequencies are obtained from a discrete time to continuous time conversion:

$$\lambda_j = \frac{1}{\Delta t}\left(\ln|\lambda_{dj}| + i\theta_{dj}\right). \tag{5}$$

wherein θ is the argument of λ_d. Eq. (5) can be re-written as:

$$\lambda_j = 2\pi\left(-\zeta_j f_j \pm if_j\sqrt{1-\zeta_j^2} \pm i\ nf_s\right). \tag{6}$$

From Eq. (6), the observed natural frequency is $f_{j_{\mathrm{obs}}} = |\lambda_j|/2\pi$. By Nyquist theorem, $f_{j_{\mathrm{obs}}} \leq f_s/2$. Re-writing Eq. (6), we get:

$$f_{j_{\mathrm{obs}}}^2 = \zeta_j^2 f_j^2 + \left(\pm f_j\sqrt{1-\zeta_j^2} \pm nf_s\right)^2. \tag{7}$$

Since damping in most machine tool systems is low [14], i.e., $\zeta \ll 1$, Eq. (7) reduces to:

$$f_{j_{\mathrm{obs}}}^2 = \left(f_j \pm nf_s\right)^2. \tag{8}$$

When $n = 0$, the signal is not aliased. However, if $f_{j_{\mathrm{obs}}} < f_j$, the signal always is. Deducing then that f_j will likely be always greater than or equal to $f_{j_{\mathrm{obs}}}$, Eq. (8) becomes:

$$f_j = \begin{cases} nf_s + f_{j_{\mathrm{obs}}} \\ nf_s - f_{j_{\mathrm{obs}}},\ n \neq 0 \end{cases}; n \in W. \tag{9}$$

Since the likely true natural frequency is evidently a function of the observed frequency, which in turn is a function of the sampling frequency, and since there are infinite feasible solutions for f_j depending on the fold n, methods to recover true parameters from observed ones is as follows.

To determine a unique f_j, we follow the method in [10] to find the intersection of two (or more) estimates of f_j obtained from two (or more) fractionally uncorrelated measurements at two (or more) different sampling frequencies. If, for example, the sampling frequencies are $f_{s,1}$ and $f_{s,2}$, then Eq. (9) becomes:

$$f_{j,1} = \begin{cases} nf_{s,1} + f_{j_{\mathrm{obs},1}} \\ nf_{s,1} - f_{j_{\mathrm{obs},1}},\ n \neq 0 \end{cases}; n \in W;$$

$$f_{j,2} = \begin{cases} nf_{s,2} + f_{j_{\mathrm{obs},2}} \\ nf_{s,2} - f_{j_{\mathrm{obs},2}},\ n \neq 0 \end{cases}; n \in W. \tag{10}$$

The likely feasible solution is the intersection of these two sets:

$$f_j \in \{\{f_{j,1}\} \cap \{f_{j,2}\}\}. \tag{11}$$

If a unique solution is not obtained from the above intersection, then an intersection of as many uncorrelated sampling frequencies as necessary must be evaluated until the solution converges towards unique frequencies.

Knowing f_j, and since damping is independent of the sampling frequency (see real part of Eq. (6)), an estimate for the true damping ratio becomes:

$$\zeta_j = -\mathrm{real}(\lambda_j)/(2\pi f_j). \tag{12}$$

Since the spatial response is uncoupled from the temporal one, the eigenvector can directly be estimated from aliased measurements [10], i.e., if the continuous time response is:

$$\mathbf{y}(s,t) = \Phi(s)\mathbf{q}(t) = \sum_{j=1}^{m}\phi_j(s)q_j(t), \tag{13}$$

wherein s is the spatial variable corresponding to the tool point, with $\phi_j(s)$ as the jth mass-normalized mode shape and $q_j(t)$ as the jth modal coordinate for m modes, even when $\mathbf{y}(s,t)$ is potentially temporally under sampled at some uniform time instants k, the spatial $\phi_j(s)$ remains unaffected, i.e., Eq. (13) will become:

$$\mathbf{y}(s,k) = \Phi(s)\mathbf{q}(k) = \sum_{j=1}^{m}\phi_j(s)q_j(k). \tag{14}$$

Since the ERA outputs the unscaled discrete time eigenvector which is different than the mass-normalized ϕ_j of our interest, ϕ_j is evaluated from Eq. (14) by assuming the modal response to be: $q_j = \phi_j(l)\tilde{q}_j$, wherein $\tilde{q}_j$ is numerically estimated from:

$$\ddot{\tilde{q}}_j(k) + 2\zeta_j\omega_j\dot{\tilde{q}}_j(k) + \omega_j^2\tilde{q}_j(k) = f_l(k), \tag{15}$$

wherein $f_l(k)$ is the measured impulse input force at location l, and ω_j and ζ_j are identified from Eq. (11) and (12). For details about procedure to estimate $\tilde{q}_j$, please see [15].

Above procedures are used to recover modal parameters from potentially temporally aliased displacements estimated from video recordings of vibrating tools. To benchmark recovered parameters with those estimated from accelerations sampled properly, Eq. (1) is

Please cite this article as: M. Law et al., Modal parameter recovery from temporally aliased video recordings of cutting tools, CIRP Annals - Manufacturing Technology (2022), https://doi.org/10.1016/j.cirp.2022.03.023

suitably modified. And, since signals are sampled properly, f_j is obtained by setting $n = 0$ in Eqs. (3-9), ζ_j is estimated from Eq. (12), and ϕ_j from Eqs. (14-15).

3. Experimental setups

An end mill and a boring bar were excited with a modal hammer and the vibrations were recorded using a Chronos 2.1 monochrome camera fitted with a 24 - 70 mm focal length lens as shown in the setups in Fig. 1. The four-fluted end mill with a diameter of 16 mm and a stick out of 126 mm was held in a hydro-grip tool holder with a HSK63 interface on a CNC milling machine. The boring bar with a diameter of 25 mm and overhang of 225 mm was mounted in a compression holder on a CNC lathe. A DC light and a white background was used in all measurements.

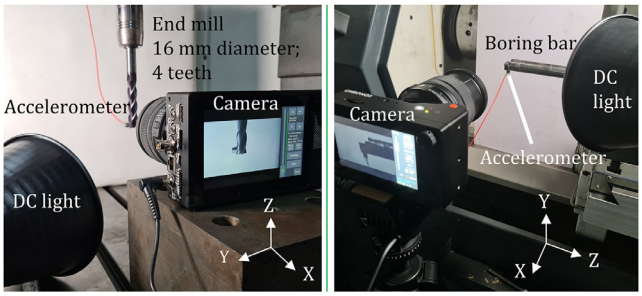

Fig. 1. Experimental setups to record tool vibrations using a camera.

Since we assume no a priori information of the modal frequencies, and since the method requires at least two measurements with uncorrelated sampling frequencies to recover parameters from potentially aliased signals, these were chosen to be 960 and 1000 frames per second, respectively, i.e., frame rates at which the resolution was 1920 × 1080, i.e., high enough such as to capture tool motion across pixels which is expected to be of the order of few tens of µm. Since we use the tool's own features to track motion across frames, image acquisition settings were adjusted to provide appropriate gradients across the tool's edge. The aperture was kept wide open. The shutter speed was set to be 500 µs, and the ISO was set to be 2000. These settings resulted in 36 µm pixels. Finer pixel resolutions might be possible with different lenses, illumination, shutter speed, and ISO settings.

Single camera setups shown in Fig. 1 can only record in-plane motion in the direction perpendicular to the edge of the tools. Methods are hence illustrated herein with the excitation and response being in the Y-direction. Out of plane motion for in plane excitation is expected to be small and is ignored. Extracted parameters were benchmarked with tool tip accelerations that were synchronously sampled at 51.2 kHz using a NI9234 DAQ with a NI9171 chassis using CutPRO®'s data acquisition module.

4. Results and discussion

4.1. Registering motion from video

MP4 video recordings were imported into MATLAB® wherein each individual frame was cropped around the edge of interest to extract tool point pixel-displacement time series data using procedures outlined in [2,3]. For two separate video sampling rates, we estimated two sets of displacements. These are used to recover parameters as discussed next.

4.2. Recovering modal parameters for the end mill

Displacement responses of the end mill along with its natural frequencies estimated using the ERA are shown in Fig. 2(a). With $f_{s,1} =$ 960 Hz, frequencies are observed at 215 Hz and at 433 Hz, and with $f_{s,2} = 1$ kHz, frequencies are at 251 Hz and at 471 Hz. Since frequencies change with sampling frequencies, the signal is aliased. Likely candidates for the natural frequencies are evaluated using Eq. (10). Their intersection (see Eq. (11)) results in the 'true' modes. For this case, the 'true' modes are evaluated to be 527 Hz, and 745 Hz. Clearly, to faithfully estimate these modes, the video should have originally been recorded at frequencies ≥2 × 745 Hz. That, however, would require the use of high-speed cameras. Methods proposed herein can avoid that.

The beating-like phenomena observed in Fig. 2(a, c) is an artefact of the observed frequencies being close to half the sampling frequencies. Though the beat frequency distorts the response, it does not influence modal parameter estimation [3].

Knowledge of the 'true' modes was used to estimate the damping using Eq. (12). And, since inputs were measured, mass-normalized eigenvectors were estimated from the modal response using Eqs. (14-15). Recovered modal parameters are listed in Table 1, which also lists those extracted from the 'ground truth' acceleration data. Results are in good agreement for the first mode. Since the second mode is dynamically stiffer, it vibrates with less magnitude than can be easily resolved with the per pixel resolution of 36 µm, and hence there are differences in the estimated frequencies (∼5%) and in the eigenvectors (∼10%). Differences can be reduced further by spatially resolving displacements by magnifying motion using different lenses or using subpixel level motion registrations schemes. These can form part of future investigations. Furthermore, since vision-based methods are full-field, methods herein can be extended to extract mode shapes of interest using procedures outlined in [2].

To demonstrate how the proposed methods can recover modal parameters from potentially aliased accelerations too, properly sampled acceleration signals shown in Fig. 2(b) (Accln. [g]) were downsampled to the same rates at which video was recorded. The corresponding response and frequencies for these cases are shown in Fig. 2(c). Since these results are from downsampled data, they are different than those from the aliased video signals. In this case, since accelerometers can measure higher frequency responses with higher fidelity, and since the properly sampled data showed both modes, the dynamically stiffer second mode with the downsampled data is also better resolved and is in closer agreement with the 'ground truth'.

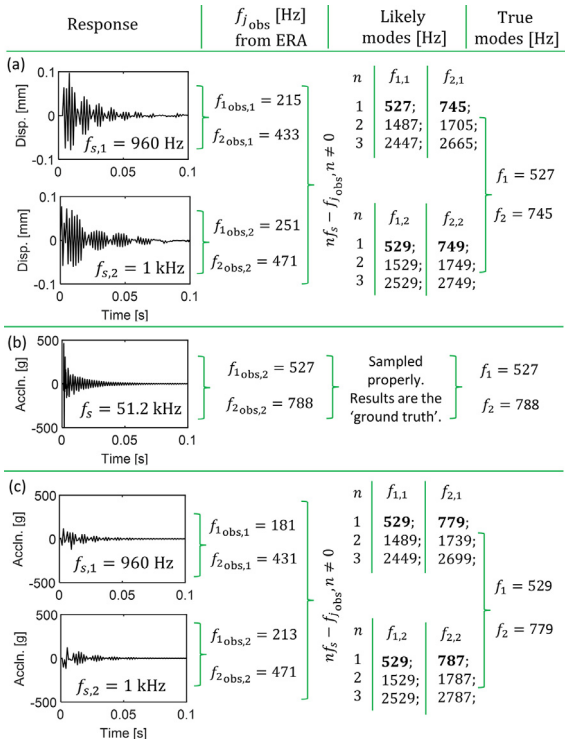

Fig. 2. Recovering end mill natural frequencies from aliased signals.

Please cite this article as: M. Law et al., Modal parameter recovery from temporally aliased video recordings of cutting tools, CIRP Annals - Manufacturing Technology (2022), https://doi.org/10.1016/j.cirp.2022.03.023

Table 1
Comparison of modal parameters for the end mill

Mode	Recovered from aliased video recordings			From accelerations sampled properly		
	f_j[Hz]	ζ_j [%]	ϕ_j	f_j [Hz]	ζ_j [%]	ϕ_j
1st	527	1.18	1.14	527	1.6	1.32
2nd	745	5.7	0.82	788	5.3	0.92

4.3. Recovering modal parameters for the boring bar

A summary of recovery of natural frequencies of the boring bar from potentially aliased displacements estimated from video is shown in Fig. 3. In this case, from the two differently sampled videos, only one frequency is estimated at 210 Hz – see Fig. 3(a), suggesting that the signal is sampled appropriately for this frequency, and this is indeed the 'true' natural frequency, as is confirmed from the estimates from accelerations sampled properly – see Fig. 3(b). Though properly sampled accelerations suggest that there is a second mode, since it is likely dynamically much stiffer than the first, it is not properly spatially resolved, and hence is not 'visible'. Damping and eigenvector for the first and dominant mode are estimated and are found to agree with those obtained from accelerations sampled properly – see Table 2.

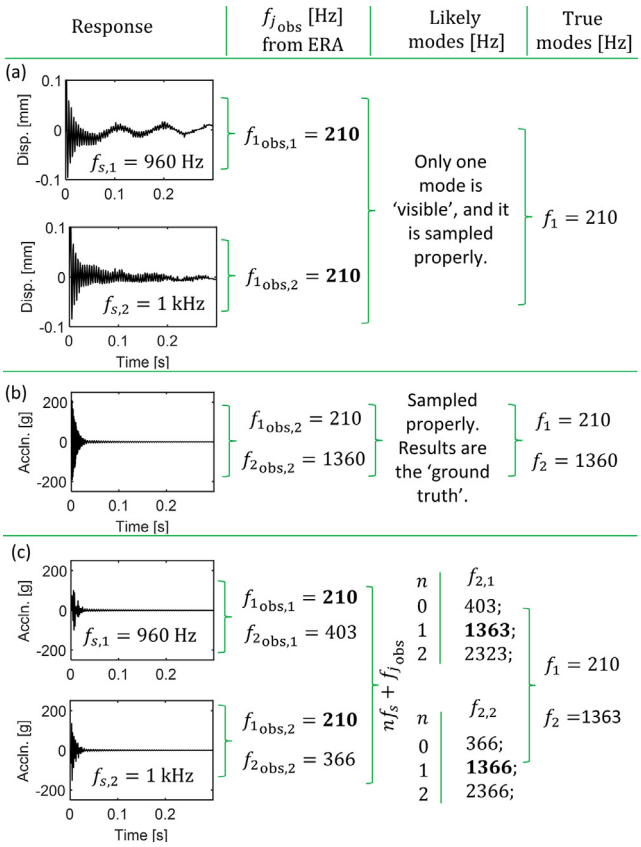

Fig. 3. Recovering boring bar natural frequencies from aliased signals.

Table 2
Comparison of modal parameters for the slender boring bar

Mode	Recovered from aliased video recordings			From accelerations sampled properly		
	f_j[Hz]	ζ_j [%]	ϕ_j	f_j [Hz]	ζ_j [%]	ϕ_j
1st	210	0.8	0.69	210	0.9	0.68
2nd	-	-	-	1360	1.7	1.7

To demonstrate again how the methods are generalizable, they are applied to accelerations downsampled to the same rate as video was recorded – see Fig. 3(c). In this case, two modes are visible, one properly, and another aliased – evident from frequencies being different with changing sampling rates. The likely mode is estimated using procedures outlined, and the 'true' mode is found to be in good agreement with the 'ground truth'.

5. Conclusions

Methods to recover modal parameters from temporally aliased video recordings of cutting tools were presented in this paper. Though there are some challenges in recovering weakly excited modes, results, in general, were found to agree well with those from accelerations sampled properly. Methods were shown to also work with downsampled acceleration signals, demonstrating their generalizability for use with other sensors.

Though two uncorrelated measurements were found adequate herein, future work could test for robustness of the method for noisy systems with different orders and for systems in which observed modes are confounded. Further developments could explore estimation of small subpixel level motion and recovery from spatiotemporally aliased signals using video recordings from cell phone cameras. Proposed methods also have implications for condition monitoring using vibration data with low sampling rates, which in turn will mean less data to transmit, store and process.

Declaration of Competing Interest

The authors declare that they have no known competing financial interests or personal relationships that could have appeared to influence the work reported in this paper.

Acknowledgements

We acknowledge Government of India's Science and Engineering Research Board's Core Research Grant CRG/2020/001010.

References

[1] Okubo N, Yoshida Y (1982) Application of modal analysis to machine tool structures. *CIRP Annals* 31(1):243–246.
[2] Law M, et al. (2020) Modal analysis of machine tools using visual vibrometry and output-only methods. *CIRP Annals* 69(1):357–360.
[3] Gupta P, et al. (2021) Vision-based modal analysis of cutting tools. *CIRP J of Manu. Sci. and Tech.* 32:91–107.
[4] Gupta P, Law M (2021) Evaluating tool point dynamics using smartphone-based visual vibrometry. *Procedia CIRP* 101:250–253.
[5] Yang Y, Nagarajaiah S (2015) Output-only modal identification by compression sensing: Non-uniform low-rate random sampling. *Mech. Syst. Signal Proc.* 56:15–34.
[6] Pang, et al. (2018) A random demodulation architecture for sub-sampling acoustic emission signals in structural health monitoring. *J. Sound Vib.* 431:390–404.
[7] Martinez B, et al. (2021) Sparse and random sampling techniques for high-Resolution, full-field, BSS-based structural dyn. identification from video. *Sensors* 20(12):3526.
[8] Bhowmick S, Nagarajaiah S (2022) Spatiotemporal compressive sensing of full-field Lagrangian continuous displacement response from optical flow of edge: Identification of full-field dynamic modes. *Mech. Syst. Signal Process* 164:108232.
[9] Barone S, et al. (2019) Low-frame-rate single camera system for 3D full-field high-frequency vibration measurements. *Mech. Syst. Signal Process* 123:143–152.
[10] Yang Y, et al. (2017) Blind identification of full-field vibration modes of output-only structures from uniformly-sampled, possibly temporally-aliased (sub-Nyquist), video measurements. *J. of Sound and Vibration* 390:232–256.
[11] Juang J, Pappa R (1985) An eigensystem realization algorithm for modal parameter identification and model reduction. *J Guidance, Control & Dyn* 8:620–627.
[12] Gupta P, et al. (2020) Evaluating tool point dynamics using output-only modal analysis with mass-change methods. *CIRP J of Manu. Sci. and Tech.* 32:91–107.
[13] Maia N M M, Silva J M M (1997) *Theoretical and experimental modal analysis*, Research Studies Press.
[14] Zaeh, et al. (2019) Predictive simulation of damping effects in machine tools. *CIRP Annals* 68(1):393–396.
[15] Mukhopadhyay, et al. (2014) Modal parameter based structural identification using input–output data: Minimal instrumentation and global identifiability issues. *Mech. Syst. Signal Process* 45:283–301.